AGU ADVANCING EARTH AND SPACE SCIENCES

Geophysical Research Letters®

Key Points:
- 80% of the CMIP models simulate a decrease of the Atlantic Niño variability at the end of the 21st century
- The model uncertainty explains about 80% of the total uncertainty on Atlantic Niño variability projections at the end of the 21st century
- Global warming signal is not detectable throughout scenarios due to large internal variability and model uncertainties

Uncertainty on Atlantic Niño Variability Projections

A. Prigent[1] , **R. A. Imbol Koungue[2]** , **A. S. N. Imbol Nkwinkwa[2]** , **G. Beobide-Arsuaga[3,4]** , and **R. Farneti[1]**

[1]Earth System Physics Section, The Abdus Salam International Centre for Theoretical Physics (ICTP), Trieste, Italy, [2]GEOMAR Helmholtz Centre for Ocean Research Kiel, Kiel, Germany, [3]International Max Planck Research School on Earth System Modelling, Hamburg, Germany, [4]Center for Earth System Research and Sustainability (CEN), Institute of Oceanography, Universität Hamburg, Hamburg, Germany

Abstract Sources of uncertainty (i.e., internal variability, model and scenario) in Atlantic Niño variability projections were quantified in 49 models participating in the Coupled Model Intercomparison Phases 5 (CMIP5) and 6 (CMIP6). By the end of the twenty-first century, the ensemble mean change in Atlantic Niño variability is −0.07 ± 0.10°C, with 80% of CMIP models projecting a decrease, and representing a 16% reduction relative to the 1981–2005 ensemble mean. Models' projections depict a large spread, with variability changes ranging from 0.23°C to −0.50°C. Internal variability is the main source of uncertainty until 2045 but model uncertainty dominates thereafter, eventually explaining up to 80% of the total uncertainty. The scenario uncertainty remains low (<1%) throughout the twenty-first century. The total uncertainty on Atlantic Niño variability projections is not improved when considering only CMIP models with a realistic zonal equatorial Atlantic sea surface temperature gradient.

Plain Language Summary Sources of uncertainty (i.e., internal variability, model and scenario) in future projections of the Atlantic Niño variability were evaluated in global coupled models participating in the Coupled Model Intercomparison Phases 5 (CMIP5) and 6 (CMIP6). Relative to 1981–2005, models' projections depict a large spread, ranging from increasing Atlantic Niño variability by up to 0.23°C to decreasing by up to −0.50°C. By the end of the twenty-first century, the ensemble mean Atlantic Niño variability change is −0.07 ± 0.10°C with 80% of the global coupled models simulating a decrease. This change in the ensemble mean Atlantic Niño variability, relative to the period 1981–2005, represents a 16% reduction. During the first four decades of projection, the internal variability is the main contributor to the total uncertainty; thereafter model uncertainty dominates and explains up to 80% of the total uncertainty at the end of the twenty-first century. The scenario uncertainty remains low (<1%) throughout the twenty-first century. The total uncertainty on Atlantic Niño variability projections is not improved when considering only CMIP models with a realistic zonal equatorial Atlantic sea surface temperature gradient.
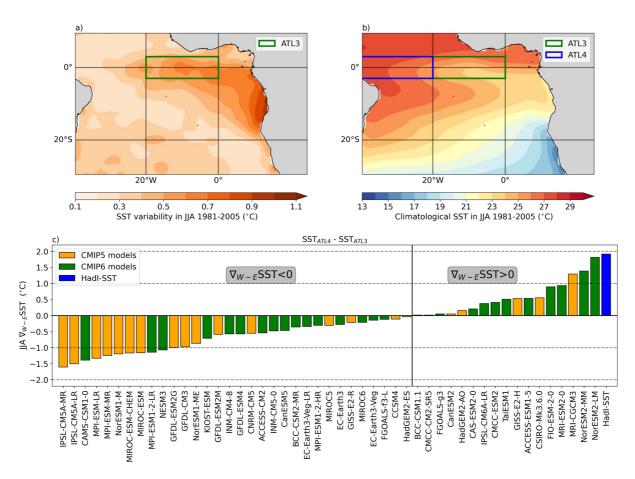
1. Introduction

The eastern equatorial Atlantic features high interannual sea surface temperature (SST) variability that strongly impacts the climate on the surrounding continents (Folland et al., 1986; Hirst and Hastenrath, 1983; Nobre & Shukla, 1996). Interannual SST variability is dominated by the Atlantic Niño mode (Lübbecke et al., 2018). The Atlantic Niño mode has its center of action in the eastern equatorial Atlantic in the ATL3 region (Zebiak, 1993; green box Figure 1a; 20°W–0°, 3°S–3°N) and preferentially peaks in boreal summer (June-July-August, JJA) when the Atlantic cold tongue develops (Figure 1b). Coupled ocean-atmosphere interactions, such as for El Niño/Southern Oscillation (ENSO) in the Pacific Ocean, are at the heart of the Atlantic Niño mechanisms (Keenlyside & Latif, 2007; Servain et al., 1982). During an Atlantic Niño event, warm SST anomalies (SSTA) develop in the ATL3 region which decrease the east-west SST gradient leading to anomalous westerlies that depress the thermocline in the east, favoring a warming there.

In the past, the variability of the Atlantic Niño mode has undergone multidecadal changes. Over the period 1960–1999, Tokinaga and Xie (2011) showed a reduction of 48% of the interannual variability of the zonal equatorial Atlantic SST gradient in root-mean-square variance. Further, Prigent et al. (2020) and Silva et al. (2021) while comparing the periods 1982–1999 to 2000–2017 and 1980–1999 to 2000–2010, respectively, reported a reduction of boreal summer SST variability of about 30%. Yet, recent studies show a resurgence of the eastern

Figure 1. (a) Standard deviation of the SSTA in JJA from HadI-SST over the tropical Atlantic (40°W–20°E; 30°S–10°N) and during the period 1981–2005. (b) Climatological HadI-SST in JJA over the tropical Atlantic and during the period 1981–2005. The green and blue boxes denote the ATL3 (20°W–0°; 3°S–3°N) and the ATL4 (40°W–20°W; 3°S–3°N) regions, respectively. (c) Zonal equatorial SST gradient in JJA, defined as the difference between the ATL4 mean SST and the ATL3 mean SST during the period 1981–2005. CMIP5 (CMIP6) models are represented by orange (green) bars and HadI-SST by a blue bar.

equatorial Atlantic interannual SST variability, with strong Atlantic Niños in 2019 (Richter et al., 2022) and 2021 (Li et al., 2023).

The future behavior of the Atlantic Niño mode under increasing greenhouse gas concentrations gained focus in recent years. Projections using climate models participating in the Coupled Model Intercomparison Project Phases 5 (CMIP5) and 6 (CMIP6), point toward a future weakening of the Atlantic Niño mode (Crespo et al., 2022; Worou et al., 2022; Yang et al., 2022). Yang et al. (2022) showed that the reduced SST variability in JJA was attributed to: a reduced equatorial zonal wind sensitivity to zonal SST gradient, due to a more stable equatorial Atlantic atmosphere; and reduced SST sensitivity to thermocline depth anomalies, due to a deepened thermocline in the eastern equatorial Atlantic. While there is a large model agreement toward a weakening of the ATL3 inter-annual SST variability, there is a substantial uncertainty on the magnitude of this change (Crespo et al., 2022). To our knowledge, no attempt has been made to quantify the sources of this large uncertainty. Identifying the contribution of the different sources (model, internal variability and scenario uncertainties) is necessary to make progress in reducing the uncertainty on future projections.

Persistent biases in the tropical Atlantic mean-state within coupled model simulations are examined as another potential source of uncertainty for future projections of the Atlantic Niño variability. The tropical Atlantic mean-state suffers from a large warm bias (Davey et al., 2002; Farneti et al., 2022; Imbol Nkwinkwa et al., 2021; Richter & Tokinaga, 2020), particularly in the east, due to too weak easterly winds, leading to the misrepresentation of the equatorial Atlantic zonal SST gradient (∇_{W-E}SST, Figure 1c) and excessively deep thermocline in the east (Richter & Xie, 2008). Yet, a few CMIP models can simulate a positive zonal equatorial SST gradient in JJA, although generally too weak in comparison to observations (Figure 1c). The main goals of this study are

threefold: (a) investigate the consistency of the projections of the Atlantic Niño variability in the CMIP models; (b) quantify the sources of uncertainties in Atlantic Niño variability projections for the twenty-first century following the methodology outlined by Beobide-Arsuaga et al. (2021) for ENSO variability projections; (c) assess the link between the mean-state biases and uncertainties on the Atlantic Niño variability projections.

2. Data and Methods

2.1. Model Data

In this study we use monthly mean data from the CMIP5 and CMIP6 models and from the variants r1i1p1 and r1p1i1f1, respectively. In total, we analyze the SST (variable name: tos) from 49 climate models, 22 from CMIP5 and 27 from CMIP6. Models' historical runs and future projections under three different scenarios, namely the Representative Concentration Pathways (RCP2.6, RCP4.5, and RCP8.5) for CMIP5 and Shared Socioeconomic Pathways (SSP1-2.6, SSP2-4.5, and SSP5-8.5; O'Neill et al., 2016) for CMIP6 are examined. While CMIP5 models are forced with historical forcing up to 2005, CMIP6 models are forced by historical forcing up to 2014. Here, for both ensembles, we define a consistent historical period from 1900 to 2005 and projection period from 2005 to 2099. CMIP models' outputs were bi-linearly interpolated on a common 1° by 1° horizontal grid. When analyzing the Bjerknes feedback (see Text S2 in Supporting Information S1), we consider the SST, the zonal wind speed at 10 m (Uwind, variable name: uas) and the sea surface height (SSH, variable name: zos) from 16 and 18 CMIP5 and CMIP6 models, respectively, under scenarios RCP2.6/SSP1-2.6, RCP4.5/SSP2-4.5, RCP8.5/SSP5-8.5 and the idealized abrupt$4 \times CO_2$ experiment. The lists of the models used and the different variables available can be found in Tables S1 and S2 in Supporting Information S1 for the CMIP5 and CMIP6 models, respectively.

2.2. Observational Data Sets and Reanalysis Products

In order to analyze the interannual SST variability over the historical period the following data sets with monthly resolution were used: the Hadley Centre Sea Ice and Sea Surface Temperature version 1.1 (HadI-SST, Rayner et al., 2003) available at 1° by 1° horizontal resolution and spanning the period 1870/01 onwards; the Ocean Reanalysis System version 5 (ORA-S5, Zuo et al., 2019) available at 0.25° by 0.25° horizontal resolution and spanning the period 1958/01 onwards; and the European Centre for Medium-range Weather Forecast Re-analysis 5 (ERA5) product (Hersbach et al., 2020) available at 0.25° by 0.25° horizontal resolution and spanning the period 1940/01 onwards.

2.3. Atlantic Niño Variability

The Atlantic Niño variability, *X*, is calculated as the 31-year running standard deviation of the JJA-averaged SSTA over the ATL3 region. The choice of the ATL3 region was made given that most CMIP5 and CMIP6 models show high interannual SST variability in this region (Figures S1 and S2 in Supporting Information S1, respectively). SSTAs are calculated over each 31-year running window as follows: (a) the ATL3-averaged SSTs are linearly detrended and (b) the ATL3 SSTA are obtained by subtracting the climatological monthly mean seasonal cycle to each running window.

2.4. Sub-Ensembles Definition

Five different sub-ensembles are defined to investigate future projections in the Atlantic Niño variability: (a) the 49 CMIP models; (b) the 22 CMIP5 models; (c) the 27 CMIP6 models; (d) the 32 CMIP models simulating a negative zonal SST gradient in the equatorial Atlantic (∇_{W-E}SST < 0, Figure 1c); and (e) the 17 CMIP models simulating a positive zonal SST gradient in the equatorial Atlantic (∇_{W-E}SST > 0, Figure 1c).

2.5. Sources of Uncertainty

The uncertainty analysis is similar to the one proposed in Beobide-Arsuaga et al. (2021) for ENSO, which is based on the studies of Hawkins and Sutton (2009) and Reintges et al. (2017). Hawkins and Sutton (2009) showed that the total uncertainty on climate predictions can be divided in three sources: internal variability (*I*), model (*M*) and scenario (*S*) uncertainties. The detailed method to derive these uncertainties can be found in Text S1

in Supporting Information S1 but a summary is provided as follows. From a second order polynomial fit of X, $X_f(s,m,t)$, we derive the long-term Atlantic Niño variability change, x_f, relative to the period 1981–2005. Using x_f we can define the time-dependent inter-model uncertainty $M(t)$. It corresponds to the spread between models' projections which are then averaged over the three scenarios:

$$M(t) = \frac{1}{N_s} \cdot \sum_s \text{var}_m(x_f(s,m,t)) \tag{1}$$

The scenario uncertainty, $S(t)$, is also time-dependent and can be defined by averaging x_f over all models for each scenario and by computing the spread among the three of them:

$$S(t) = \text{var}_s\left(\frac{1}{N_m} \sum_m x_f(s,m,t) \right) \tag{2}$$

Next, the internal variability, I, is estimated by taking the spread of each model's internal variability, $\varepsilon(s,m,t) = X(s,m,t) - X_f(s,m,t)$, over time and then averaging over all models and scenarios:

$$I = \frac{1}{N_s} \cdot \sum_s \frac{1}{N_m} \cdot \sum_m \text{var}_t(\varepsilon(s,m,t)) \tag{3}$$

It follows that the total uncertainty, $T(t)$, is given by:

$$T(t) = M(t) + S(t) + I \tag{4}$$

3. Global Warming Signal of the Atlantic Niño Variability and Its Uncertainties

The global warming signal of the Atlantic Niño variability ($x_f(s,m,t)$, see Text S1 in Supporting Information S1) is shown in Figure 2 for the different sub-ensembles. Unlike Beobide-Arsuaga et al. (2021), where a disagreement in ENSO variability projections was observed, there is a large agreement toward a reduction of the Atlantic Niño variability, consistent with previous findings (Crespo et al., 2022; Worou et al., 2022; Yang et al., 2022). In the following, we discuss the changes in the Atlantic Niño variability in boreal summer and their ranges at the end of the twenty-first century relative to 1981–2005 in function of the sub-ensembles. Out of 49 CMIP5 and CMIP6 simulations, 39, 36, and 38 (∼80%, ∼73% and ∼78%) show a reduction of the variability of the Atlantic Niño (Figure 2a) for the scenarios RCP2.6/SSP1-2.6, RCP4.5/SSP2-4.5, and RCP8.5/SSP5-8.5, respectively. Changes in the scenario mean of the Atlantic Niño variability are: −0.06 ± 0.09°C, −0.07 ± 0.11°C, and −0.08 ± 0.12°C with ranges going from −0.25°C to 0.18°C, from −0.40°C to 0.15°C and from −0.50°C to 0.23°C for RCP2.6/SSP1-2.6, RCP4.5/SSP2-4.5, and RCP8.5/SSP5-8.5. When considering only the CMIP5 models (Figure 2b): 15, 15, and 16 out of the 22 models show a decrease of the Atlantic Niño variability for the RCP2.6, RCP4.5 and RCP8.5 scenarios, respectively. The change in the Atlantic Niño variability for the CMIP5 models is −0.05 ± 0.11°C, −0.06 ± 0.12°C, and −0.08 ± 0.15°C with ranges going from −0.25°C to 0.18°C, −0.40°C to 0.13°C, and from −0.50°C to 0.23°C for RCP2.6, RCP4.5, and RCP8.5, respectively. For the CMIP6 models (Figure 2c): 24, 21 and 22 out of the 27 CMIP6 models show a reduction of the Atlantic Niño variability for the scenarios SSP1-2.6, SSP2-4.5 and SSP5-8.5, respectively. Changes in the scenario mean of the Atlantic Niño variability for the CMIP6 models are: −0.08 ± 0.07°C, −0.08 ± 0.10°C, and −0.08 ± 0.10°C with ranges going from −0.25°C to 0.02°C, from −0.26°C to 0.15°C, and from −0.24°C to 0.14°C for SSP1-2.6, SSP2-4.5, and SSP5-8.5, respectively. When considering the CMIP models with a negative zonal SST gradient in 1981–2005 (∇_{W-E}SST < 0, Figure 2d), 24, 20, and 23 of the 32 models show a decrease of the Atlantic Niño variability for the scenarios RCP2.6/SSP1-2.6, RCP4.5/SSP2-4.5, and RCP8.5/SSP5-8.5, respectively. Changes in the scenario mean of the Atlantic Niño variability for the ∇_{W-E}SST < 0 sub-ensemble are −0.04 ± 0.08°C, −0.04 ± 0.10°C and −0.06 ± 0.11°C with ranges going from −0.22°C to 0.19°C, from −0.36°C to 0.14°C, and from −0.34°C to 0.21°C for the scenarios RCP2.6/SSP1-2.6, RCP4.5/SSP2-4.5, and RCP8.5/SSP5-8.5, respectively. Finally, when considering the ∇_{W-E}SST > 0 sub-ensemble, 15, 16, and 15 out of the 17 models project a reduction of the Atlantic Niño variability (Figure 2e) for the scenarios RCP2.6/SSP1-2.6, RCP4.5/SSP2-4.5, and RCP8.5/SSP5-8.5, respectively. Changes in the scenario mean of the Atlantic Niño variability for the ∇_{W-E}SST > 0 sub-ensemble are −0.10 ± 0.08°C, −0.12 ± 0.09°C, and −0.11 ± 0.13°C with ranges going from −0.25°C to 0.05°C, from −0.31°C

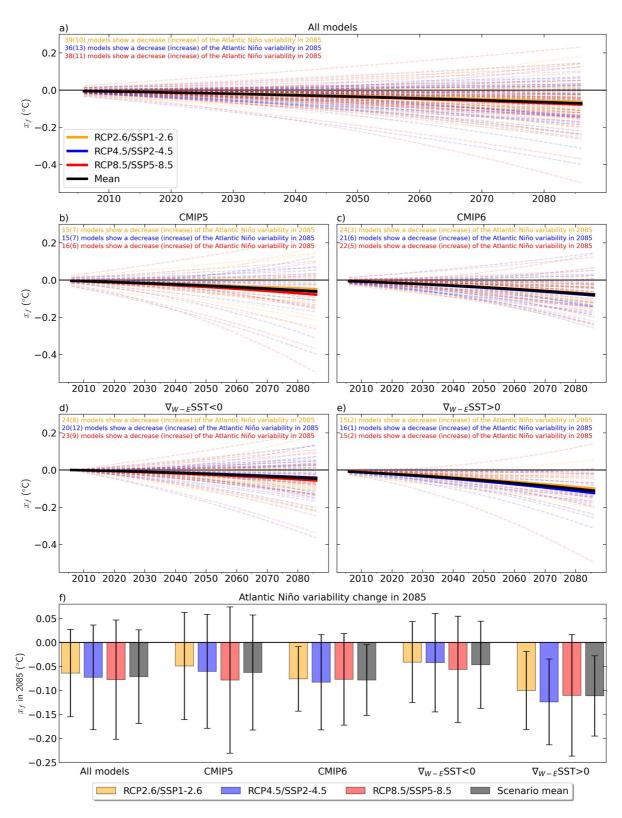**Figure 2.**

to 0.01°C and from −0.50°C to 0.14°C for the scenarios RCP2.6/SSP1-2.6, RCP4.5/SSP2-4.5 and RCP8.5/SSP5-8.5, respectively. Figure 2f summarizes scenario means of the Atlantic Niño variability change at the end of the twenty-first century for each sub-ensemble. For all sub-ensembles and scenarios, the Atlantic Niño variability is decreasing at the end of the twenty-first century. According to a Student's t-test the future changes in Atlantic Niño variability for the CMIP5 and the ∇_{W-E}SST < 0 sub-ensembles are not significant at the 95% level. Whereas the projected reduction in Atlantic Niño variability for the CMIP6 and the ∇_{W-E}SST > 0 sub-ensembles are significant at the 95% level.

We next identify and quantify the main sources of uncertainty in the Atlantic Niño variability projections (Figure 3, Text S1 in Supporting Information S1). When considering all CMIP models, the total uncertainty increases from 0.0023°C^2 in 2005 to 0.0144°C^2 at the end of the twenty-first century. In the first four decades, the main source of uncertainty is the internal variability (Figures 3a and 3b; blue) which corresponds to 97% of the total uncertainty in 2005. After 2045, the model uncertainty (Figures 3a and 3b; gray) becomes the main source of uncertainty. At the end of the projection, the model uncertainty corresponds to 84% of the total uncertainty. The scenario uncertainty (Figures 3a and 3b; purple) remains low until the end of the projection as it represents less than 1% of the total uncertainty.

We repeat the uncertainty analysis for the different sub-ensembles separately (Figure 3c). From 2005 (not shown) to 2085 (Figure 3c) sub-ensembles show that the total uncertainty ($T(t)$) increases from 0.0025°C^2 to 0.02°C^2 (CMIP5), from 0.0021°C^2 to 0.0102°C^2 (CMIP6), from 0.0019°C^2 to 0.0123°C^2 (∇_{W-E}SST < 0) and from 0.0028°C^2 to 0.0138°C^2 (∇_{W-E}SST > 0), respectively. Model uncertainty is the largest contributor to the total uncertainty at the end of the twenty-first century as it represents 87%, 79%, 84%, and 79% of the total uncertainty for CMIP5, CMIP6, ∇_{W-E}SST < 0 and ∇_{W-E}SST > 0 sub-ensembles, respectively. This indicates that some improvements have been made from CMIP5 to CMIP6 and that reducing the model uncertainty is essential to increase the confidence in future projections of Atlantic Niño variability. The signal-to-noise ratio (SNR) at the end of the twenty-first century (Figure 3d) does not exceed the value of unity for any sub-ensemble, which indicates that a global warming signal in Atlantic Niño variability cannot be detected with high statistical significance using this method. Yet, the CMIP6 and ∇_{W-E}SST > 0 sub-ensembles show a greater SNR with ratios of 0.47 and 0.58 at the end of the twenty-first century, respectively.

Finally, the low scenario uncertainty $S(t)$ is further investigated by examining the change in standard deviation of the JJA-averaged SSTA as well as the Bjerknes feedback (See Text S2 in Supporting Information S1) for the CMIP models and for each scenario (Figure 4). The CMIP ensemble mean displays a gradual reduction of the equatorial Atlantic interannual SST variability in JJA as the strength of the emission scenario increases (Figures 2f and 4a–4d), consistent with previous results (Crespo et al., 2022; Yang et al., 2022).

The three components of the Bjerknes feedback were evaluated for each scenario in order to understand the changes in interannual SST variability (Figures 4e–4g and Figures S5–S7 in Supporting Information S1, respectively). Consistent with the gradual reduction of the interannual SST variability in the ATL3 region as a function of the emission scenario, we observe a gradual decrease of the first and third Bjerknes feedback components (Figures 4e and 4g; Figures S5 and S7 in Supporting Information S1). No consistent changes are observed for the second Bjerknes feedback component (Figure 4f; Figure S6 in Supporting Information S1). This result agrees with Crespo et al. (2022) and Yang et al. (2022) who concluded that the projected change in Atlantic Niño variability is mainly linked to a reduction of the first and third Bjerknes feedback components.

4. Summary and Discussion

The global warming signal in the projected Atlantic Niño variability and corresponding uncertainties have been assessed employing CMIP5 and CMIP6 models and using a similar method as in Beobide-Arsuaga et al. (2021) for ENSO. The five sub-ensembles analyzed agree on a future reduction of the Atlantic Niño variability,

Figure 2. Global warming signal of the Atlantic Niño variability in JJA for the period 2005 to 2085 (x_f, see Text S1 in Supporting Information S1), estimated by subtracting the historical long-term trend (1981–2005) to the projected long-term trend (2005–2085). Each dashed line represents one simulation. The dashed orange, blue and red lines are the individual simulations forced by the scenarios RCP2.6/SSP1-2.6, RCP4.5/SSP2-4.5, and RCP8.5/SSP5-8.5, respectively. The thick orange, blue and red lines are the scenario means. The black line is the mean over all simulations and scenarios. All models, CMIP5 models, CMIP6 models, models with a negative and with a positive zonal equatorial SST gradient in JJA over the period 1981–2005 are considered in (a–e) respectively. (f) Bar plot showing the Atlantic Niño variability change at the end of the projected long-term trend (2085) in function of the sub-ensemble and of the scenario. The black bar represents the scenario mean.
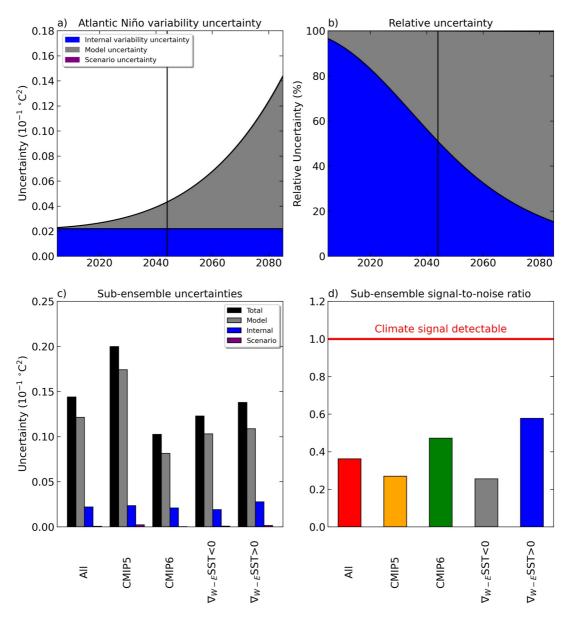
Figure 3. (a) Uncertainty of the Atlantic Niño variability for the period 2005 to 2085 for all 49 CMIP5 and CMIP6 models together divided into model (gray), internal variability (blue) and scenario uncertainty (purple). (b) Relative uncertainty for the period 2005–2085. Solid vertical black lines indicate where model uncertainty becomes larger than internal variability uncertainty, year 2045. (c) Total (black), model (gray), internal variability (blue) and scenario (purple) uncertainty at the end of the projection, year 2085 for: all 49 models, 22 CMIP5 models, 27 CMIP6 models, 32 (17) CMIP models with a negative (positive) zonal equatorial SST gradient in JJA during 1981–2005. (d) Signal-to-noise ratio (SNR), see Equation 9 in Text S1 of the Supporting Information S1, for: all models (red), CMIP5 (orange) and CMIP6 models (green), CMIP models with a negative (positive) JJA SST gradient during 1981–2005 in gray (blue). The red horizontal line indicates that the SNR is = 1.
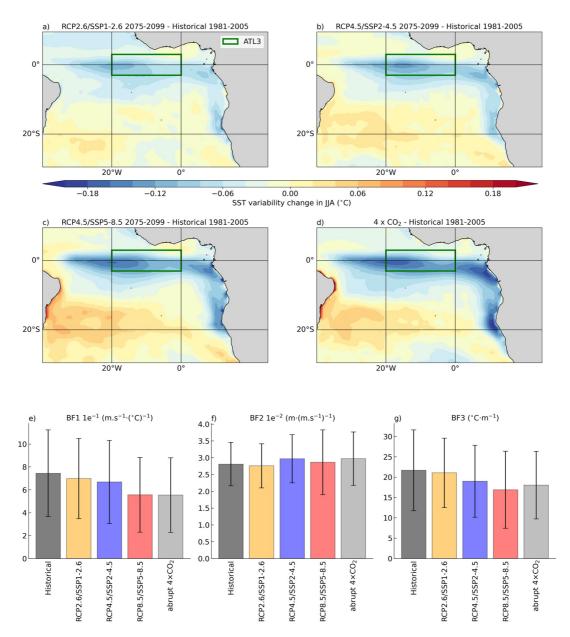
consistent with previous studies (Crespo et al., 2022; Worou et al., 2022; Yang et al., 2022). Projected changes in Atlantic Niño variability range from 0.23°C to −0.50°C with the mean global warming signal averaged over all models and scenarios of −0.07 ± 0.10°C. This is in contrast to ENSO projections, whose ensemble mean variability change was found to be close to zero (Beobide-Arsuaga et al., 2021). Furthermore, the $\nabla_{W-E}SST > 0$ sub-ensemble displays the strongest decrease in the Atlantic Niño variability with an ensemble mean reduction of −0.11 ± 0.08°C. This indicates that models with a realistic zonal SST gradient simulate a stronger decrease of the eastern equatorial Atlantic interannual SST variability.

Despite the large model consensus toward a decline of the Atlantic Niño mode over the twenty-first century, large uncertainties remain. When considering all CMIP models, the total uncertainty increases from 0.0023°C² in 2005 to 0.0144°C² in 2085 (Figure 3a). The resurgence of tropical Atlantic interannual SST variability observed in the

Figure 4. Projected SST variability change and Bjerknes feedback in JJA. (a–c) Change in the ensemble mean standard deviation of the JJA-averaged SSTA over the period 2075–2099 relative to the historical period 1981–2005 for the scenarios RCP2.6/SSP1-2.6, RCP4.5/SSP2-4.5 RCP8.5/SSP5-8.5. (d) Same as (a–c) but for the ensemble mean standard deviation of the SSTA for the abrupt4 $\times$ CO_2 experiment over a 25-year period after a 100-year spin-up. (e) ATL4 zonal wind anomalies sensitivity to ATL3 SSTA in JJA for each scenario. (f) ATL3 SSH anomalies sensitivity to ATL4 zonal wind anomalies in JJA for each scenario. (g) ATL3 SSTA sensitivity to ATL3 SSH anomalies in JJA for each scenario. Ensemble means are composed of 34 models, 16 CMIP5 and 18 CMIP6 models (Tables S1 and S2 in Supporting Information S1), for which the variables tos, uas, and zos are available for each scenario.

last years could be due to internal variability, whose uncertainty dominates until 2045 in CMIP models. Thereafter, model uncertainty is the largest contributor on the projection of the variability of the Atlantic Niño mode, explaining about 80% of the total uncertainty at the end of the twenty-first century. The large model uncertainty (i.e., intermodel discrepancies in the Atlantic Niño variability change) can be related to the different SST biases and thermocline feedback change shown by models (Crespo et al., 2022). When considering the sub-ensembles, the CMIP6 ensemble has a smaller total uncertainty in 2085 compared to the CMIP5 ensemble because of its reduced model uncertainty (Figure 3). The opposite result was found for ENSO amplitude projections, and it was linked to the larger scenario uncertainty in the CMIP6 ensemble compared to CMIP5 (Beobide-Arsuaga et al., 2021). The comparison of the uncertainty on the projection of the Atlantic Niño variability between the

sub-ensembles ∇_{W-E}SST > 0 and ∇_{W-E}SST < 0 reveals that CMIP models with a more realistic zonal equatorial Atlantic SST gradient depict larger total uncertainty. This difference in total uncertainty is explained by larger model uncertainty and internal variability in the ∇_{W-E}SST > 0 sub-ensemble. We note that the number of members in the two sub-ensembles is different and that it might influence the result. Nonetheless, this result suggests that simulating a more realistic zonal equatorial Atlantic SST gradient in the CMIP models is not sufficient to considerably reduce the large uncertainty on future Atlantic Niño variability projections.

The low scenario uncertainty (S(t) < 1%, Figure 3) in the Atlantic Niño variability projection was also investigated. In contrast to projected ENSO variability, all scenario means (RCP2.6/SSP1-2.6, RCP4.5/SSP2-4.5, and RCP8.5/SSP5-8.5) agree on a decrease in the Atlantic Niño variability. In the case of ENSO variability projections, Beobide-Arsuaga et al. (2021) found a slight increase or no change for the scenarios RCP8.5/SSP5-8.5 and RCP4.5/SSP2-4.5, respectively. When considering all CMIP models, the response of the interannual SST variability in JJA to stronger emission scenarios is consistent: stronger emission scenarios result in stronger reduction of the interannual SST variability (Figures 2f and 4). Yet, when considering the sub-ensembles CMIP6 and ∇_{W-E}SST > 0, the reduction in the Atlantic Niño variability is larger for the scenario RCP4.5/SSP2-4.5 than for RCP8.5/SSP5-8.5.

Future changes in equatorial Atlantic interannual SST variability could also arise from tropical basin interactions. ENSO and the Indian Ocean Dipole (IOD) are suggested to influence the equatorial Atlantic variability at different time scales (Chang et al., 2006; Latif and Gröztner, 2000; Zhang & Han, 2021). For this purpose, cross-correlations between SSTA averaged in ATL3 and NINO3.4 and in ATL3 and the IOD index were computed from HadI-SST and CMIP models for the historical (1981–2005) and future projections (2075–2099) for each scenario, and they are shown in Figure S8 in Supporting Information S1. Over the historical period, and in contrast to HadI-SST, CMIP models exhibit a wide range of interactions between the equatorial Atlantic, Pacific and Indian variabilities, indicating a poor representation of tropical basin interactions by CMIP models. As a result, future projections of these interactions are largely uncertain (Figure S8 in Supporting Information S1). An improved understanding and simulation of tropical basin interactions in CMIP models will help assessing their future behavior, potential impact on equatorial Atlantic variability, and in further reducing the uncertainty on Atlantic Nino variability projections.

Data Availability Statement

The CMIP6 data can be found at https://esgf-data.dkrz.de/search/cmip6-dkrz/. The CMIP5 data is publicly available at https://esgf-data.dkrz.de/search/cmip5-dkrz/. The ERA5 data used in this study can be found at https://cds.climate.copernicus.eu/cdsapp#!/dataset/reanalysis-era5-single-levels-monthly-means?tab=form. The ORA-S5 data is available at https://cds.climate.copernicus.eu/cdsapp#!/dataset/reanalysis-oras5?tab=form. The HadI-SST is publicly available at https://www.metoffice.gov.uk/hadobs/hadisst/.

References

Beobide-Arsuaga, G., Bayr, T., Reintges, A., & Latif, M. (2021). Uncertainty of ENSO-amplitude projections in CMIP5 and CMIP6 models. *Climate Dynamics*, *56*(11–12), 3875–3888. https://doi.org/10.1007/s00382-021-05673-4

Chang, P., Fang, Y., Saravanan, R., Ji, L., & Seidel, H. (2006). The cause of the fragile relationship between the Pacific El Niño and the Atlantic Niño. *Nature*, *443*(7109), 324–328. https://doi.org/10.1038/nature05053

Crespo, L. R., Prigent, A., Keenlyside, N., Koseki, S., Svendsen, L., Richter, I., & Sánchez-Gómez, E. (2022). Weakening of the Atlantic Niño variability under global warming. *Nature Climate Change*, *12*(9), 822–827. https://doi.org/10.1038/s41558-022-01453-y

Davey, M., Huddleston, M., Sperber, K., Braconnot, P., Bryan, F., Chen, D., et al. (2002). STOIC: A study of coupled model climatology and variability in tropical ocean regions. *Climate Dynamics*, *18*(5), 403–420. https://doi.org/10.1007/s00382-001-0188-6

Farneti, R., Stiz, A., & Ssebandeke, J. B. (2022). Improvements and persistent biases in the southeast tropical Atlantic in CMIP models. *npj Climate and Atmospheric Science*, *5*(1), 42. https://doi.org/10.1038/s41612-022-00264-4

Folland, C. K., Palmer, T. N., & Parker, D. E. (1986). Sahel rainfall and worldwide sea temperatures, 1901–1985. *Nature*, *320*(6063), 602–607. https://doi.org/10.1038/320602a0

Hawkins, E., & Sutton, R. (2009). The potential to narrow uncertainty in regional climate predictions. *Bulletin of the American Meteorological Society*, *90*(8), 1095–1107. https://doi.org/10.1175/2009BAMS2607.1

Hersbach, H., Bell, B., Berrisford, P., Hirahara, S., Horányi, A., Muñoz-Sabater, J., et al. (2020). The ERA5 global reanalysis. *Quarterly Journal of the Royal Meteorological Society*, *146*(730), 1999–2049. https://doi.org/10.1002/qj.3803

Hirst Antrony, C., & Hastenrath, S. (1983). Atmosphere-ocean mechanisms of climate anomalies in the Angola-Tropical Atlantic sector. *Journal of Physical Oceanography*, *13*(7), 1146–1157. https://doi.org/10.1175/1520-0485(1983)013%3c1146:aomoca%3e2.0.co;2

Imbol Nkwinkwa, A. S. N., Latif, M., & Park, W. (2021). Mean-state dependence of CO_2-forced tropical Atlantic sector climate change. *Geophysical Research Letters*, *48*, e2021GL093803. https://doi.org/10.1029/2021GL093803

Keenlyside, N. S., & Latif, M. (2007). Understanding equatorial Atlantic interannual variability. *Journal of Climate*, *20*(1), 131–142. https://doi.org/10.1175/jcli3992.1

Latif, M., & Grötzner, A. (2000). The equatorial Atlantic oscillation and its response to ENSO. *Climate Dynamics*, *16*(2–3), 213–218. https://doi.org/10.1007/s003820050014

Li, X., Tan, W., Hu, Z.-Z., & Johnson, N. C. (2023). Evolution and prediction of two extremely strong Atlantic Niños in 2019–2021: Impact of Benguela warming. *Geophysical Research Letters*, *50*(12), e2023GL104215. https://doi.org/10.1029/2023GL104215

Lübbecke, J. F., Rodríguez-Fonseca, B., Richter, I., Martín-Rey, M., Losada, T., Polo, I., & Keenlyside, N. S. (2018). Equatorial Atlantic variability—Modes, mechanisms, and global teleconnections. *Wiley Interdiscip Rev Climate Change*, *9*(4), 1–18. https://doi.org/10.1002/wcc.527

Nobre, P., & Shukla, J. (1996). Variations of sea surface temperature, wind stress, and rainfall over the Tropical Atlantic and South America. *Journal of Climate*, *9*(10), 2464–2479. https://doi.org/10.1175/1520-0442(1996)009<2464:vosstw>2.0.co;2

O'Neill, B. C., Tebaldi, C., van Vuuren, D. P., Eyring, V., Friedlingstein, P., Hurtt, G., et al. (2016). The scenario model intercomparison project (ScenarioMIP) for CMIP6. *Geoscientific Model Development*, *9*, 3461–3482. https://doi.org/10.5194/gmd-9-3461-2016

Prigent, A., Lübbecke, J., Bayr, T., Latif, M., & Wengel, C. (2020). Weakened SST variability in the tropical Atlantic Ocean since 2000. *Climate Dynamics*, *54*(5–6), 2731–2744. https://doi.org/10.1007/s00382-020-05138-0

Rayner, N. A., Parker, D. E., Horton, E. B., Folland, C. K., Alexander, L. V., Rowell, D. P., et al. (2003). Global analyses of sea surface temperature, sea ice, and night marine air temperature since the late nineteenth century. *Journal of Geophysical Research*, *108*, 4407. https://doi.org/10.1029/2002JD002670

Reintges, A., Martin, T., Latif, M., & Keenlyside, N. S. (2017). Uncertainty in twenty-first century projections of the Atlantic Meridional Overturning circulation in CMIP3 and CMIP5 models. *Climate Dynamics*, *49*(5–6), 1495–1511. https://doi.org/10.1007/s00382-016-3180-x

Richter, I., & Tokinaga, H. (2020). An overview of the performance of CMIP6 models in the tropical Atlantic: Mean state, variability, and remote impacts. *Climate Dynamics*, *55*(9–10), 2579–2601. https://doi.org/10.1007/s00382-020-05409-w

Richter, I., Tokinaga, H., & Okumura, Y. M. (2022). The extraordinary equatorial Atlantic warming in late 2019. *Geophysical Research Letters*, *49*(4), e2021GL095918. https://doi.org/10.1029/2021GL095918

Richter, I., & Xie, S. P. (2008). On the origin of equatorial Atlantic biases in coupled general circulation models. *Climate Dynamics*, *31*(5), 587–598. https://doi.org/10.1007/s00382-008-0364-z

Servain, J., Picaut, J., & Merle, J. (1982). Evidence of remote forcing in the equatorial Atlantic Ocean. *Journal of Physical Oceanography*, *12*(5), 457–463. https://doi.org/10.1175/1520-0485(1982)012%3c0457:eorfit%3e2.0.co;2

Silva, P., Wainer, I., & Khodri, M. (2021). Changes in the equatorial mode of the tropical Atlantic in terms of the Bjerknes feedback index. *Climate Dynamics*, *56*(9–10), 3005–3024. https://doi.org/10.1007/s00382-021-05627-w

Tokinaga, H., & Xie, S. P. (2011). Weakening of the Equatorial Atlantic cold tongue over the past six decades. *Nature Geoscience*, *4*(4), 222–226. https://doi.org/10.1038/ngeo1078

Worou, K., Goosse, H., Fichefet, T., & Kucharski, F. (2022). Weakened impact of the Atlantic Niño on the future equatorial Atlantic and Guinea Coast rainfall. *Earth System Dynamics*, *13*(1), 231–249. https://doi.org/10.5194/esd-13-231-2022

Yang, Y., Wu, L., Cai, W., Jia, F., Ng, B., Wang, G., & Geng, T. (2022). Suppressed Atlantic Niño/Niña variability under greenhouse warming. *Nature Climate Change*, *12*(9), 814–821. https://doi.org/10.1038/s41558-022-01444-z

Zebiak, S. E. (1993). Air–Sea interaction in the equatorial Atlantic region. *Journal of Climate*, *6*(8), 1567–1586. https://doi.org/10.1175/1520-0442(1993)006h1567:AIITEAi2.0.CO;2

Zhang, L., & Han, W. (2021). Indian Ocean Dipole leads to Atlantic Niño. *Nature Communications*, *12*(1), 5952. https://doi.org/10.1038/s41467-021-26223-w

Zuo, H., Balmaseda, M. A., Tietsche, S., Mogensen, K., & Mayer, M. (2019). The ECMWF operational ensemble reanalysis–analysis system for ocean and Sea Ice: A description of the system and assessment. *Ocean Science*, *15*(3), 779–808. https://doi.org/10.5194/os-15-779-2019

References From the Supporting Information

Bjerknes, J. (1969). Atmospheric teleconnections from the equatorial Pacific. *Monthly Weather Review*, *97*(3), 163–172. https://doi.org/10.1175/1520-0493(1969)097<0163:ATFTEP>2.3.CO;2

Meinshausen, M., Nicholls, Z. R. J., Lewis, J., Gidden, M. J., Vogel, E., Freund, M., et al. (2020). The shared socio-economic pathway (SSP) greenhouse gas concentrations and their extensions to 2500. *Geoscientific Model Development*, *13*(8), 3571–3605. https://doi.org/10.5194/gmd-13-3571-2020

Meinshausen, M., Smith, S. J., Calvin, K., Daniel, J. S., Kainuma, M. L. T., Lamarque, J.-F., et al. (2011). The RCP greenhouse gas concentrations and their extensions from 1765 to 2300. *Climatic Change*, *109*(1–2), 213–241. https://doi.org/10.1007/s10584-011-0156-z